Kochi Chapter

Indian Geotechnical Conference
IGC 2022
15th – 17th December, 2022, Kochi

Kinematic SSI Effect on Foundation Input Motions for Building with Subterranean Levels

Zeleke Lulayehu Tadesse[1, 3] [0000-0001-9815-9527], Hari Krishna Padavala[1] [0000-0002-4581-0555], and Venkata R. P. Koteswara[2] [0000-0001-7098-1674]

[1] Department of Civil Engineering, National Institute of Technology, Warangal, Telangana 506 004, India
[2] Department of Civil Engineering, Vardhaman College of Engineering, Hyderabad, Telangana 501 518, India
[3] Faculty of Civil Engineering, Arba Minch Institute of Technology, Arba Minch, SNNPR, Ethiopia
zeleke@student.nitw.ac.in

Abstract. The substructure approach to the solution of seismic soil-structure interaction (SSI) problems becomes more convenient particularly when analytical or semi-analytical methods can be employed. Applying this approach, the seismic response studies of structures are often performed by replacing the surrounding and foundation soils with dynamic impedance functions under the excitation of foundation input motion (FIM). The presence of embedded modules of the building system may modify noticeably the FIM. The two primary objectives of this study are to assess the impact of kinematic interaction on FIM and to evaluate the applicability range of theoretical models for kinematic SSI response analyses. Numerous three-dimensional (3D) nonlinear dynamic response analyses were carried out in ABAQUS for different embedment depths, subsoil conditions, and seismic input motion on a medium-rise building with subterranean levels. The results of the numerical models reveal that when the depth of subterranean levels is increased, the characteristic and value of the FIM is considerably varied with respect to the free-field motion. It was also observed that the numerical modeling methods can predict more reliably incorporating different combination of effects and nonlinearity, particularly in lower period and higher embedment. Theoretical models, however, were failed to capture the effects of deeply embedded subterranean levels and nonlinearity behavior of subsoil profile, as well as the frequency-dependent attenuation or intensification of the subterranean level motion.

Keywords: Soil-Structure Interaction (SSI), Subterranean Levels, Foundation Input Motion, Kinematic Interaction, Transfer Function Models.

1 Introduction

The dynamic response of building structures are often influenced by the intricate interaction between the structural system and the compliant subsoil. This complex mechanism of seismic SSI resulting from kinematic interaction, which is due to the presence of non-rigid but stiff massless subterranean components on or in soil modifies the FIM, as well as inertial interaction, in which again the FIM is further modified by inertia-driven forces also often referred to as D'Alembert forces acting in the structural system. The former is the focus of this study, in particular the FFM disturbances caused on by the presence of embedded subterranean levels. The kinematic interaction response is essentially a result

of the difference in deformation and stiffness characteristics between the subterranean components and soil stratum, which is the concept of kinematic SSI. Seismic response analysis of building structures supported on compliant foundations often uses a substructure method, in which the subterranean components mostly soil is not explicitly incorporated, but rather are replaced by foundation impedance (springs and dashpots), and the analyses are carried out under the excitation of foundation level input ground motion. The ground motion is suitable for input to the foundation-level or free end of the springs, also referred to as the foundation input motion (FIM).

For deeply embedded foundations, the kinematic interaction response is more noticeable compared to shallow foundations [1]. In the case of building structures with one or more subterranean levels, the characteristics and magnitude of the FIM may be influenced by the presence of embedded subterranean modules. It can be a result of the kinematic interaction effect induced by an embedded stiff subterranean component of the structural system [2] and the nonlinearity effect [3] and causes the FIM to diverge noticeably from the FFM. Therefore, the ground motion at the foundation level obtained from kinematic interaction response analyses corresponds to an FFM that needs modification to account for the effects of kinematic SSI before being applied as base excitation to the system.

Although a thorough and comprehensive nonlinear SSI analysis can simulating soil-structure systems with a high degree of accuracy [4], routine design requires a considerable amount of computational skill and time. Hence, depending on the significance of the structure, simplified approaches are applied. Spectral reduction factors or transfer functions are two straightforward techniques for estimating the FIM for embedded foundations. Both take into account the frequency-dependent change in the FFM. Transfer functions are frequently used to evaluate the variation of ground motions caused by embedded rigid massless foundations, which describe the ratio in the frequency/time domain of the amplitude of the Fourier transforms of the FIM (u_{FIM}) to the surface FFM, (u_g). In the past, several analytical models in the literature have been presented addressing the filtering issue to estimate the transfer function for a massless circular and rectangular shape rigid foundation, embedded in a homogeneous linear soil profile or viscoelastic half-space [2, 5–9]. These analytical expressions can be utilized to estimate the modified motions at the foundation level of a building compared with FFM, and vice-versa. More recently, using both numerical and theoretical models [10–11], as well as utilizing real signal recordings from the instrumented buildings with a basement [12–13], analytical expressions were also developed relating intensity and frequency content records between the ground surface and the foundation level motions.

In this work, finite element based models are utilized for three-dimensional (3D) SSI analyses using a direct-based numerical method. In this context, several 3D finite element seismic SRA were performed for different embedment depths of subterranean levels (i.e., 1, 3, and 5 basement stories), soil profiles (soft, medium, and stiff homogeneous soil deposit), and seismic input motion of the soil-structure system in ABAQUS [14]. Since inertial effects are disregarded, the transfer function only depicts the effect of kinematic interaction. Transfer function models are often expressed by the translational and rotational components of the FFM. However, when the foundation embedment depth to width ratio (D/B) is low, as it is for the building adopted in this study, the rotational component is not considered to be significant. Hence, only the translational components of the translation functions of numerical solutions were considered in this study.

2 Soil-structure interaction analysis

2.1 Structure-foundation-soil system under investigation

A fifteen-story reinforced concrete moment-resisting frame (RC-MRF) building regular in plan (Fig. 1(a)) and elevation (Fig. 1(b)) representing the conventional medium-rise type of buildings is adopted as a reference for this work. The columns of the building are supported by an embedded mat foundation with one, three, and five basement floor systems (Fig. 2), resting on a homogenous different soil profiles underline by rigid bedrock (Table 3). The building was designed according to the Indian standard IS 456 [15] in a relatively high-risk earthquake-prone zone-V response spectra.

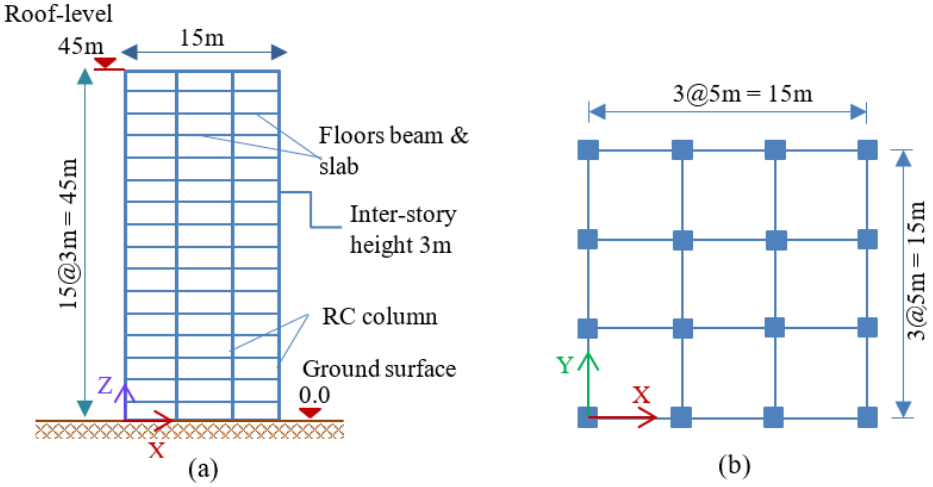

Fig. 1. The layout of the fifteen-story RC-MRF building adopted in the study: (a) superstructure elevation view, and (b) standard floor plan of the building.

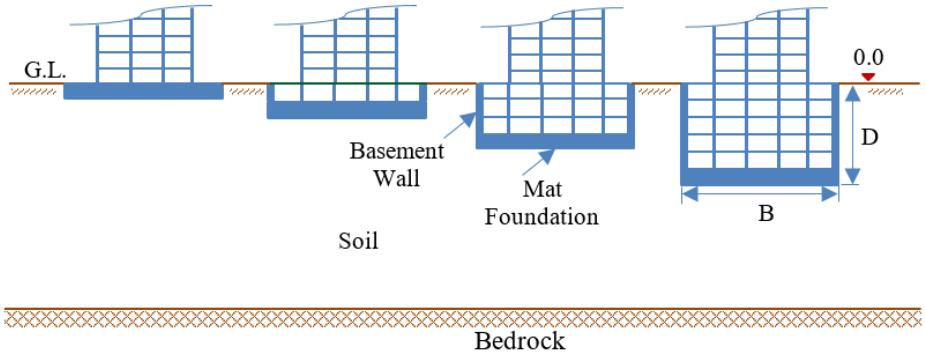

Fig. 2. Schematics of the subterranean levels embedment cases with 0BS, 1BS, 3BS, and 5BS.

In accordance with standard engineering design procedures (IS 456 [15], Bowles [16]), the mat foundation was designed to sustain the static and dynamic

loads of the structure, to meet the requirements for maximum settlement and bearing capacity, whereas the integrated basement walls were intended to support the lateral earth pressure, the shear and bending moment. The material characteristics and designed sections for the building structural elements are presented in Table 1 and Table 2, respectively.

Table 1. Characteristics of adopted concrete and steel reinforcement in structural designs.

Concrete grade	Steel reinforcement grade	Elastic modulus, E (kPa)	Poisson's ratio, ν
M30 (f'_c = 30MPa)	Fe415 (f_y = 415MPa)	27386.13	0.2

Table 2. Designed sections for the building's structural elements.

Storey Level	Basement	1 - 3	4 - 6	7 - 9	10 - 12	13 - 15
Column(m^2)	65x65	60x60	55x55	50x50	45x45	40x40
Beam (m^2)	65x35	65x35	60x35	55x35	50x35	45x35
Floor slab, t_s (m)	Basement wall, t_w (m)			Foundation, t_f (m)		
0.15	0.25			1		

Table 3. Engineering properties of the soil considered in this study ([17][18]).

Soil type	USCS	$V_{S,30}$ (m/s)	G_{max} (MPa)	ρ (kg/m^3)	E (MPa)	ν	SPT	PI (%)	C' (kN/m^2)	ϕ' (°)
C[a] / I[b]	GM, SM	600	623.4	1765	1608.3	0.28	N > 50	-	5	40
D[a] / II[b]	CL	320	177.3	1716	484.9	0.39	30	20	20	19
E[a] / III[b]	CL	150	33.1	1470	91.7	0.40	6	15	20	12

[a] ASCE 7-10 [19], [b] IS 1893:2000 [20], USCS – unified soil classification system

2.2 Seismic input motion

In the present study, the Christchurch, New Zealand earthquake acceleration record (Fig. 3 and Table 4) was considered for seismic dynamic response analysis. This earthquake ground motion was incorporated into the numerical simulation while carrying out a non-linear time history analysis. The chosen earthquake ground motion is FFM. In the assessment of transfer functions, besides standard baseline and filtering correction, significant windowing and smoothing signal processing may be required [21].

Table 4. Details of earthquake ground motion data considered for the present study.

Earthquake Event	Year	Mw (R)	PGA (g)	Duration (sec)
Christchurch, New Zealand	2011	6.2	0.371	49.985

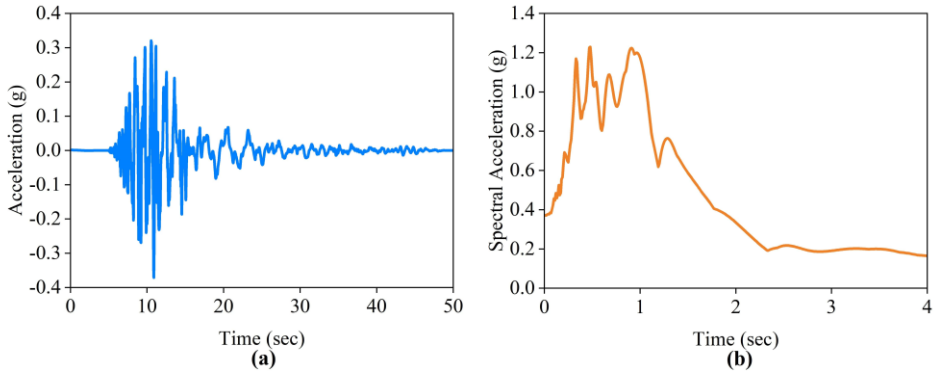

Fig. 3. Christchurch - New Zealand earthquake record 2011 (a) free-field acceleration time history, and (b) the corresponding response spectra.

2.3 Numerical kinematic SSI analysis

In this assessment, applying a direct approach as illustrated in Fig. 4 a 3D full dynamic response analyses were carried out with the numerical method in ABAQUS (Fig. 5). Since the structural system seismic response analysis is not the aim of the investigation, the structural members were modeled to behave elastically. The soil model, however, was the only one given the ability to capture nonlinear seismic responses.

The structural frame elements and basement walls were modeled using standard one-dimensional beam elements and two-dimensional shell elements, whereas the foundation element was simulated with 3D solid elements, assuming a linear elastic isotropic behavior for all elements of the structural system. The most important properties of the structural system used in this study are presented in Table 1 and Table 2. As observed in the literature, some of the past SRA is carried out by introducing rigid systems within the embedment depth of the subterranean system, disregarding the superstructure. In this study differently, the massless superstructure system also was modeled properly taking into account the system stiffness [10].

The 3D finite element soil medium was modeled with 3D stress element C3D8R (8-noded linear brick, reduced integration, hourglass control), whereas to avoid multiple reflections during the dynamic response analyses, to reduce a special dimension of the soil medium, as well as to optimize the computational effort, the far field soil domain was modeled with 3D 8-node linear one-way infinite brick (CIN3D8) elements [22](Fig. 4 and Fig. 5). As suggested by [23], the bottom of the soil medium (bedrock) was simulated using a rigid boundary condition, while the excitation motion was applied at the bedrock levels and propagating upwards through the entire model. Through sensitivity analysis, a soil domain with an extent of greater than 7B in the longitudinal direction was considered, where B is the width of the foundation. As observed by some numerical and experimental tests [24], and also suggested by modern seismic resistance design codes (FEMA 450 [25], ATC-40 [26]) the most local site amplification occurs within the top 30m of the soil deposit; thus, the vertical extent (bedrock depth) of the finite element soil models were limited to 30m in this study.

The 3D numerical model of the soil profile was simulated as nonlinear elastic-plastic material using the Mohr-Coulomb failure criterion. The profiles were examined in the

nonlinear elastoplastic constitutive model that considered viscous damping (Rayleigh damping). The Rayleigh damping matrix [C] is as given in Eq. (1), which has a linear combination of mass-proportional and stiffness-proportional components used in the analysis according to Ryan and Polanco [27].

$$[C] = \alpha[M] + \beta[K] \tag{1}$$

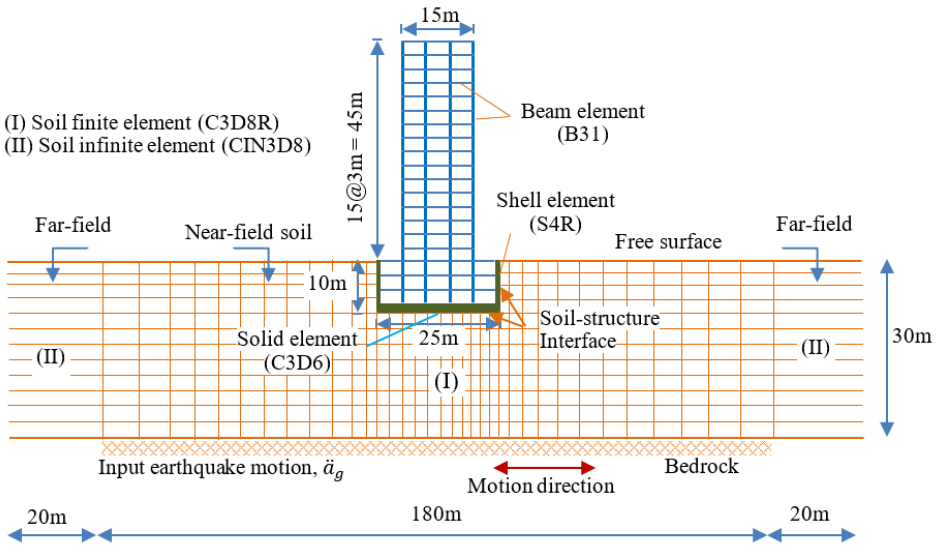

Fig. 4. The direct method configuration used for modeling the integrated soil-structure system of a 15-stories building with three subterranean levels.

where [M] and [K] are the mass and stiffness matrices of the soil, respectively; α and β are the model coefficients, chosen to specify the model damping ratio in two modes. Table 5 represents the natural frequencies of the soil profiles and the corresponding Rayleigh damping coefficients estimated for the first four modes.

Table 5. Fundamental frequencies and Rayleigh damping coefficients of the soil profiles.

Soil type	Frequency (Hz)				Rayleigh damping coefficients	
	f_1	f_2	f_3	f_4	α	β
C	5	15	25	35	2.3562	0.0008
D	2.67	8	13.33	18.67	1.2566	0.0015
E	1.250	3.750	6.250	8.750	0.5890	0.0032

In most numerical dynamic SSI analyses the size of elements mainly depends on the geometry of the embedded component of the structural system and loading conditions (static or dynamic). The element sizes are often refined near the targeted area to take into account the severe stress gradients and plasticity encountered in the soil medium, whereas a gradual transition to a coarser element considers far from the targeted area in lateral

directions of the soil medium. To describe correctly the minimum wavelength of the applied signals, the maximum size, h_{max}, of the elements was estimated using Eq. (2) in this study.

$$h_{max} \leq \frac{1}{a} \times \lambda \tag{2}$$

where, $\lambda = Vs / f_{max}$, in which V_S = the soil smallest shear wave velocity of interest, f_{max} = maximum frequency of interest, and a = 5, 8, and 10 as per [28], [29], and [30], respectively.

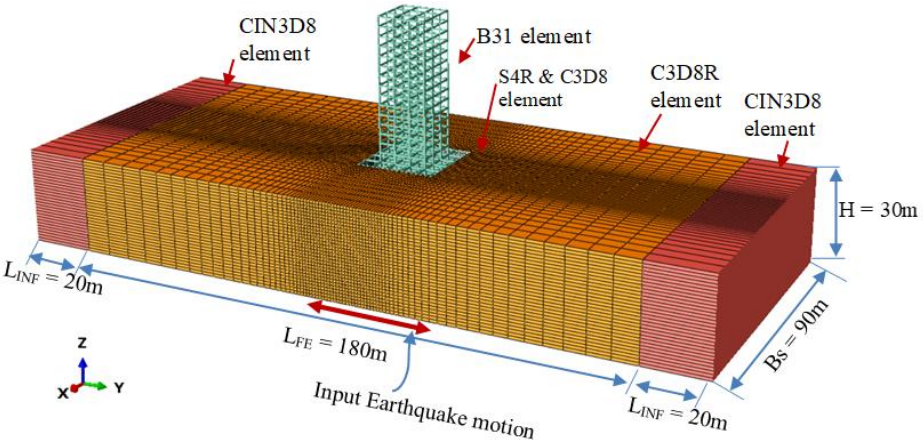

Fig. 5. The integrated soil-structure system with the adopted 3D finite element model.

2.4 Transfer function models

In this study, two translational transfer function models were adopted from the literature to evaluate the applicability range of such closed-form solutions for SSI response analysis. The first model is the one reported by NIST [1]. The horizontal foundation translation transfer function component is expressed in NIST as given in Eq. (3).

$$I_u\left(\frac{\omega D}{V_s}\right) = \frac{u_{FIM}}{u_g} = \begin{cases} cos\left(\frac{\omega D}{V_s}\right), & \frac{\omega D}{V_s} < 1.1 \\ 0.45, & \frac{\omega D}{V_s} > 1.1 \end{cases} \tag{3}$$

The other transfer function model evaluated in this assessment is the simple analytical expression proposed by Conti et al. [11] for rigid massless and massive embedded foundations (Eq. 4). This is an improved version of Eq. (3) taking into account the normalized parameters such as B/D, $\omega D/V_S$, and ρ_F/ρ_S.

$$\left|I_u\left(\frac{B}{D}, \frac{\rho_F}{\rho_s}, \frac{\omega D}{V_s}\right)\right| = \frac{a_1}{\sqrt{1 + \left(\frac{\rho_F}{\rho_s} \cdot \frac{\omega D}{V_s}\right)^2}} + \frac{(1 - a_1)}{\left[1 + \left(\frac{\omega D}{V_s}\right)^2\right]^{a_1 a_3}} \cdot \left|cos\left(a_2 \frac{\omega D}{V_s}\right)\right| \tag{4}$$

where a_1, a_2 and a_3 are the coefficients depending on the ratio B/D and ρ_F/ρ_S whose expressions are described in [11]. ρ_F and ρ_S are foundation and soil mass densities.

3 Results and Discussion

The impact of kinematic SSI on FIM for building structures with varying subterranean levels in wide-ranging subsurface conditions has been evaluated using a thorough parametric investigation. The seismic response of the soil-foundation-structure system is evaluated for vertically propagating shear waves. The ground motion is defined at the top of bedrock level or bottoms of the soil deposit. Transfer functions are evaluated at the top of the mat foundation.

3.1 Seismic site response analysis

One-dimensional equivalent linear de-convolution analysis in the frequency domain and three-dimensional nonlinear convolution analysis in the time domain were carried out in DEEPSOIL [31] and ABAQUS, respectively, to verify the accuracy of the selected element size settings in the finite element model for simulation of wave propagation [32]. The shear modulus and damping reduction curves were obtained using Vucetic and Dobry [33] classical formulas. Fig. 6 presents the comparison of the results obtained from the two analyses of soil type E/III and a reasonably good matching was observed throughout the entire period.

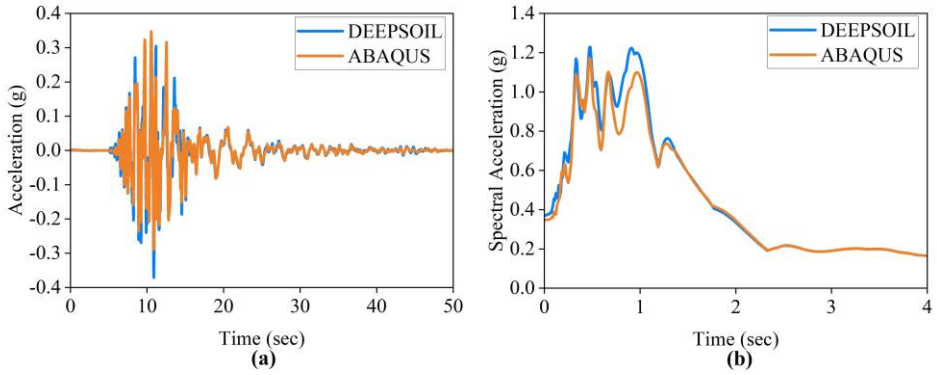

Fig. 6. (a) free-field motion, and (b) the corresponding 5% damping response spectra.

3.2 Influence of foundation embedment and soil properties on FIM

In the present assessment, the variations of foundation level motion at the building in various embedments and nonlinear soil profiles are presented in Fig. 7 in terms of transfer functions. The kinematic interaction response analyses results as shown in Fig. 7(i) the motion at the foundation level of a building decreases (i.e., $I_u < 1$) within the period ranges between 0.2 to 1s as the basement level depth increases, whereas in contrast more intense than the FFM (i.e., $I_u = 1$) particularly at lower periods and for deeper embedment depths. Similarly, as presented in Fig. 7(ii) the effect of soil properties on FIM exhibits the same characteristics as the stiffness of the soil properties decreases from stiff soil to soft soil.

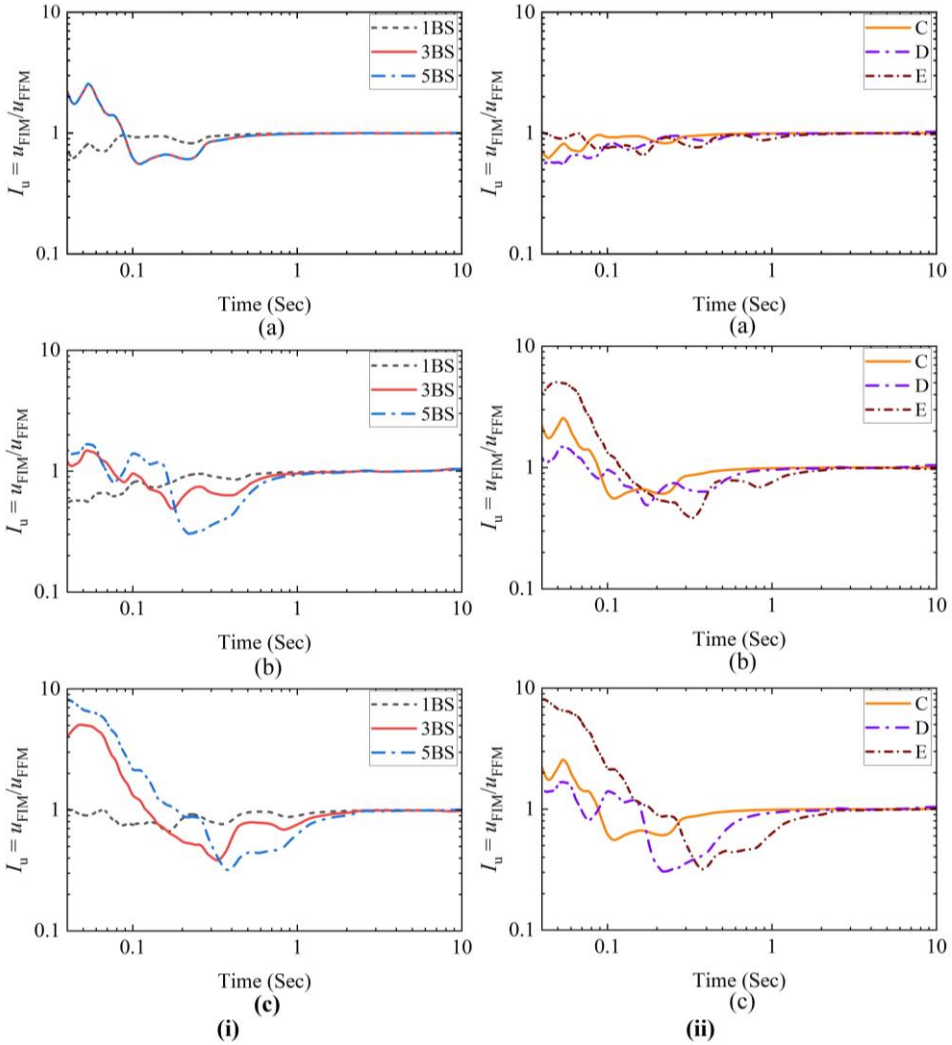

Fig. 7. Effect of (i) embedment into different soil profiles on the FIM: (a) soil type C, (b) soil type D, (c) soil type E, and (ii) soil profiles into various subterranean levels on the FIM; (a) 1BS, (b) 3BS, and (c) 5BS.

3.3 Analytical and numerical based solutions of transfer functions

The analytical transfer function models presented by NIST [1] and Conti et al. [11] were compared to the numerical finite element solutions. Fig. 8, Fig. 9 & Fig. 10 shows the analytical and nonlinear soil model numerical solutions of transfer functions at different subterranean levels in various soil profiles. It has been seen that the analytical models assessed create similar transfer functions that only diverge at lower durations. The numerical solution of the transfer function match can be considered satisfactory, having small divergences only emerge at lower periods. For the higher subterranean level in low stiff soil profiles, the mismatch is more noticeable, especially within a small time range.

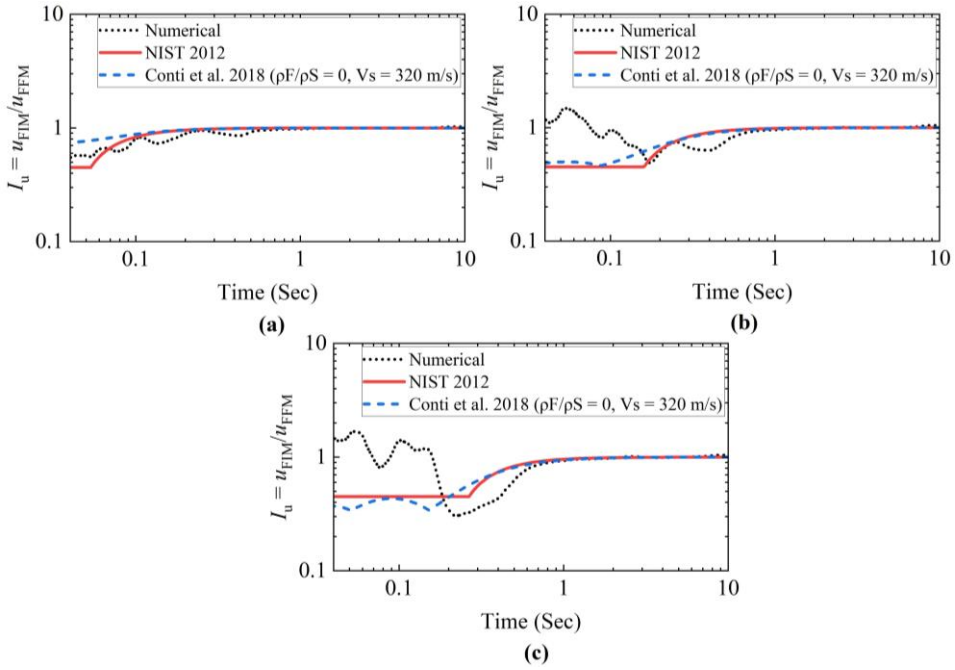

Fig. 8. Transfer functions obtained from analytical solutions and nonlinear soil model numerical solutions in soil type C for (a) 1BS, (b) 3BS, and (c) 5BS.

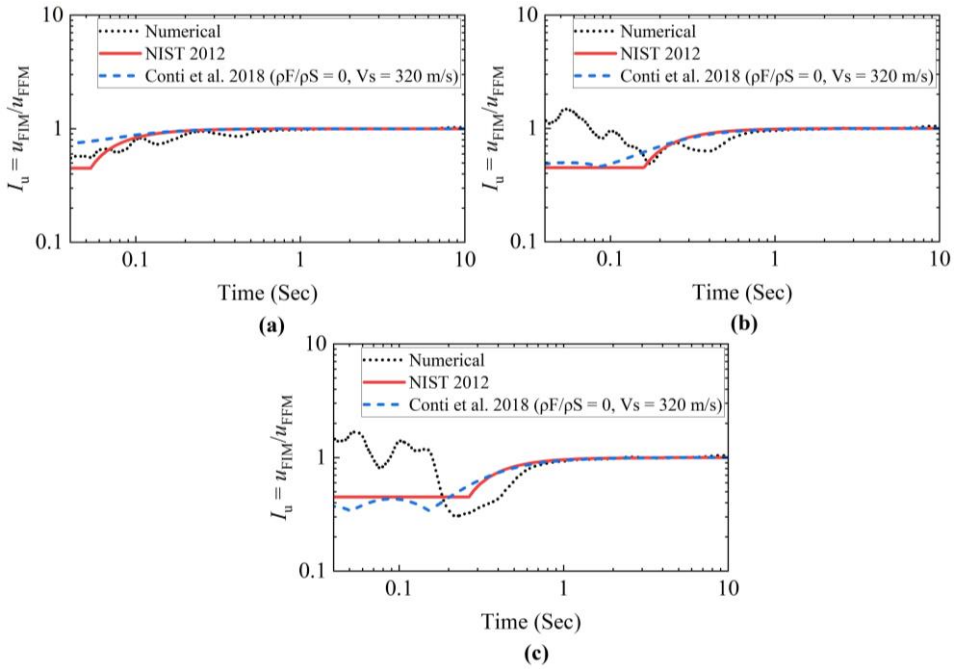

Fig. 9. Transfer functions obtained from analytical solutions and nonlinear soil model numerical solutions in soil type D for (a) 1BS, (b) 3BS, and (c) 5BS.

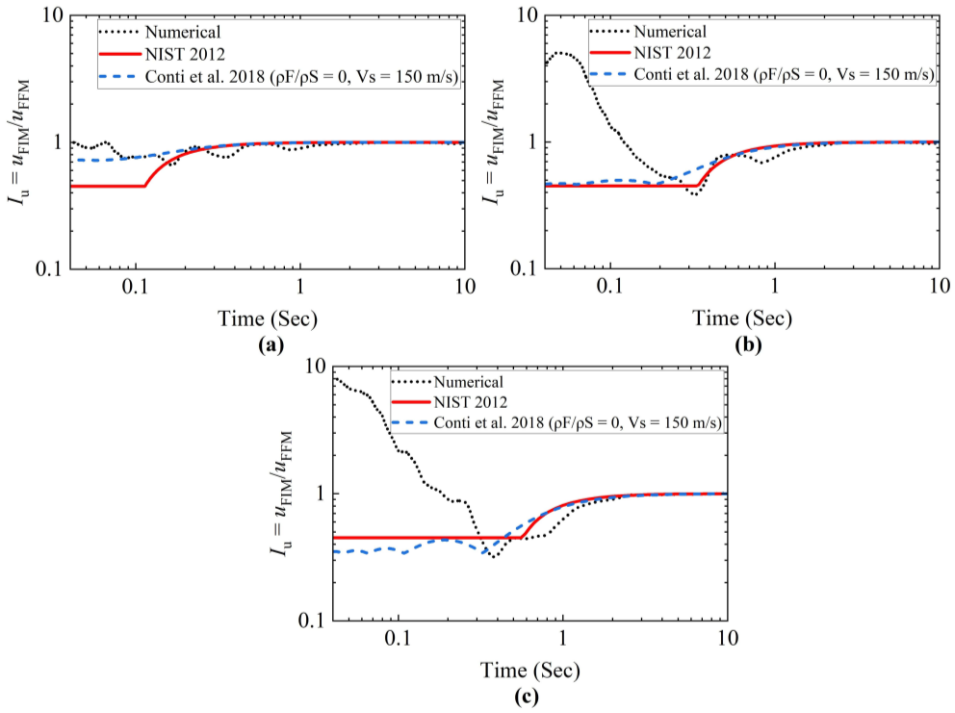

Fig. 10. Transfer functions obtained from analytical solutions and nonlinear soil model numerical solutions in soil type E for (a) 1BS, (b) 3BS, and (c) 5BS.

Conclusions

This paper assessed the effect of kinematic SSI on FIM and the applicability of the two theoretical transfer function models often used in the literature for seismic response analyses of building with subterranean levels using the substructure method. Several nonlinear detailed 3D dynamic response analyses were performed for different soil profiles featuring on top a fifteen-story RC-MRF building with subterranean levels having varied embedment depths under excitation of bedrock level earthquake motion. The variations of the motion at the foundation level of a building in various embedments and nonlinear soil profiles were evaluated in terms of transfer functions. The motion at the foundation level of a building decreases within the period range between 0.2 to 1s as the depth increases, whereas in contrast more intense than the FFM revealed particularly at lower periods for deeper embedment depths. Similarly, the effect of soil properties on FIM exhibits the same characteristics as the stiffness of the soil properties decreases from stiff soil to soft soil. Furthermore, the applicability range of analytical transfer function models was also compared with numerical model results. The results appeared to reveal that analytical models can only reliably predict the effects of embedment. Considerable variances, on the other hand, are noticed for the presence of deep subterranean levels. The models properly anticipate a constant transfer function value for higher periods, which is consistent with the numerical analyses, whereas the divergence is more significant, especially within a small time range. It was also observed that the numerical modeling methods can predict more

reliably incorporating different combination of effects and nonlinearity, particularly in lower period and higher embedment. Theoretical models, however, were failed to capture the effects of deeply embedded subterranean levels and nonlinearity behavior of subsoil profile, as well as the frequency-dependent attenuation or intensification of the subterranean level motion.

References

[1] NIST, "Soil-Structure Interaction for Building Structures," 2012.

[2] F. Elsabee and J. P. Morray, "Dynamic Behavior of Embedded Foundations," *Massachusetts Inst. Technol. Dep. Civ. Eng. Constr. Facil. Div.*, 1977.

[3] J. P. Stewart, "Variation between foundation-level and free-field earthquake ground motions," *Earthq. Spectra*, vol. 16, no. 2, pp. 511–532, 2000.

[4] D. Pitilakis, M. Dietz, D. M. Wood, D. Clouteau, and A. Modaressi, "Numerical simulation of dynamic soil-structure interaction in shaking table testing," *Soil Dyn. Earthq. Eng.*, vol. 28, no. 6, pp. 453–467, 2008, doi: 10.1016/j.soildyn.2007.07.011.

[5] S. M. Day, "Seismic response of embedded foundations," 1978.

[6] J. Dominguez and J. M. Roesset, *Response of embedded foundations to travelling waves*. 1978.

[7] D. L. Karabalis and D. E. Beskos, "Dynamic response of 3-D embedded foundations by the boundary element method," *Comput. Methods Appl. Mech. Eng.*, vol. 56, no. 1, pp. 91–119, 1986, doi: 10.1016/0045-7825(86)90138-6.

[8] J. E. Luco and H. L. Wong, "Seismic response of foundations embedded in a layered half-space," *Earthq. Eng. Struct. Dyn.*, vol. 15, no. 2, pp. 233–247, 1987, doi: 10.1002/eqe.4290150206.

[9] A. Mita and J. E. Luco, "Impedance functions and input motions for embedded square foundations," *J. Geotech. Eng.*, vol. 115, no. 4, pp. 491–503, 1989, doi: 10.1061/(ASCE)0733-9410(1989)115:4(491).

[10] R. Conti, M. Morigi, and G. M. B. Viggiani, "Filtering effect induced by rigid massless embedded foundations," *Bull. Earthq. Eng.*, vol. 15, no. 3, pp. 1019–1035, 2017, doi: 10.1007/s10518-016-9983-7.

[11] R. Conti, M. Morigi, E. Rovithis, N. Theodoulidis, and C. Karakostas, "Filtering action of embedded massive foundations: New analytical expressions and evidence from 2 instrumented buildings," *Earthq. Eng. Struct. Dyn.*, vol. 47, no. 5, pp. 1229–1249, 2018, doi: 10.1002/eqe.3014.

[12] D. Sotiriadis, N. Klimis, B. Margaris, and A. Sextos, "Influence of structure – foundation – soil interaction on ground motions recorded within buildings," *Bull. Earthq. Eng.*, vol. 17, no. 11, pp. 5867–5895, 2019, doi: 10.1007/s10518-019-00700-6.

[13] D. Sotiriadis, N. Klimis, B. Margaris, and A. Sextos, "Analytical expressions relating free-field and foundation ground motions in buildings with basement, considering soil-structure interaction," *Eng. Struct.*, vol. 216, p. 110757, 2020.

[14] A. Duval *et al.*, "Abaqus/CAE 6.14 User's Manual," *Dassault Systémes Inc. Provid. RI, USA*, vol. IV, pp. 1–6, 2014.

[15] IS 456, "Code of practice for plain and reinforced concrete (third revision)," *Bur. Indian Stand. New Dehli*, pp. 1–114, 2000.

[16] J. E. Bowles, *Foundation Analysis and Design*. 1997.

[17] A. Massumi and H. R. Tabatabaiefar, "Effects of Soil-Structure Interaction on Seismic Behaviour of Ductile Reinforced Concrete Moment Resisting Frames," *Proc. World Hous. Congr. Afford. Qual. Hous.*, 2007.

[18] S. H. Reza Tabatabaiefar, B. Fatahi, and B. Samali, "Seismic Behavior of Building Frames Considering Dynamic Soil-Structure Interaction," *Int. J. Geomech.*, vol. 13, no. 4, pp. 409–420, 2013, doi: 10.1061/(asce)gm.1943-5622.0000231.

[19] ASCE/SEI 7-10, *Minimum Design Loads for Buildings and Other Structures*. 2010.

[20] IS 1893 (Part 1), "Criteria for Earthquake resistant design of structures,Part 1:General Provisions and buildings," *Bur. Indian Stand. New Delhi*, vol. 1893, pp. 1–44, 2016.
[21] A. Mikami, J. P. Stewart, and M. Kamiyama, "Effects of time series analysis protocols on transfer functions calculated from earthquake accelerograms," *Soil Dyn. Earthq. Eng.*, vol. 28, no. 9, pp. 695–706, 2008, doi: 10.1016/j.soildyn.2007.10.018.
[22] O. C. Zienkiewicz, C. Emson, and P. Bettess, "A novel boundary infinite element," *Int. J. Numer. Methods Eng.*, vol. 19, no. 3, pp. 393–404, 1983, doi: 10.1002/nme.1620190307.
[23] B. Fatahi and S. H. R. Tabatabaiefar, "Fully Nonlinear versus Equivalent Linear Computation Method for Seismic Analysis of Midrise Buildings on Soft Soils," *Int. J. Geomech.*, vol. 14, no. 4, p. 04014016, 2014, doi: 10.1061/(asce)gm.1943-5622.0000354.
[24] M. H. Rayhani and M. H. El Naggar, "Numerical Modeling of Seismic Response of Rigid Foundation on Soft Soil," *Int. J. Geomech.*, vol. 8, no. 6, pp. 336–346, 2008, doi: 10.1061/(asce)1532-3641(2008)8:6(336).
[25] FEMA 450, "NEHRP Recommended Provisions for Seismic Regulations for New Buildings and Other Structures," *Part 1*, p. 338, 2003.
[26] ATC 40, "Seismic evaluation and retrofit of concrete buildings (Report No. ATC-40)," *Appl. Technol. Counc. Redw. City, California, USA*, 1996.
[27] K. L. Ryan and J. Polanco, "Problems with Rayleigh Damping in Base-Isolated Buildings," *J. Struct. Eng.*, vol. 134, no. 11, pp. 1780–1784, 2008, doi: 10.1061/(asce)0733-9445(2008)134:11(1780).
[28] ASCE/SEI 4-98, "Seismic analysis of safety-related nuclear structures," 1998.
[29] R. L. Kuhlemeyer and J. Lysmer, "Finite Element Method Accuracy for Wave Propagation Problems," *Journal of the Soil Mechanics and Foundations Division*, vol. 99, no. 5. pp. 421–427, 1973. doi: 10.1061/jsfeaq.0001885.
[30] ASCE/SEI 4-16, *Seismic analysis of safety-related nuclear structures*, vol. 4. 2017. doi: 10.1061/9780784413937.
[31] Y. M. A. Hashash *et al.*, "DEEPSOIL 7.0, User Manual," *Urbana, IL, Board Trust. Univ. Illinois Urbana-Champaign*, no. 2020, pp. 1–170, 2020.
[32] V. R. Feldgun, Y. S. Karinski, D. Z. Yankelevsky, and A. V. Kochetkov, "A new analytical approach to reconstruct the acceleration time history at the bedrock base from the free surface signal records," *Soil Dyn. Earthq. Eng.*, vol. 85, pp. 19–30, 2016, doi: 10.1016/j.soildyn.2016.03.003.
[33] M. Vucetic and R. Dobry, "Effect of soil plasticity on cyclic response," *J. Geotech. Eng.*, vol. 117, no. 1, pp. 89–107, 1991.